

1

## Supporting Information

### 2 **Atomistic Structure Generation of Covalent Triazine-Based** 3 **Polymers by Molecular Simulation**

4 Ce Song,<sup>ac</sup> Fangyuan Hu,<sup>\*b</sup> Zhaoliang Meng,<sup>a</sup> Shengming Li,<sup>d</sup> Wenlong Shao,<sup>c</sup>

5 Tianpeng Zhang,<sup>b</sup> Siyang Liu,<sup>b</sup> and Xigao Jian<sup>\*abc</sup>

6

7 <sup>a</sup> *School of Mathematical Sciences, Dalian University of Technology, No.2 Linggong*

8 *Road, Gaoxin District, Dalian, Liaoning, China. E-mail: jian4616@dlut.edu.cn*

9 <sup>b</sup> *School of Materials Science and Engineering, State Key Laboratory of Fine*

10 *Chemicals, Dalian University of Technology, No.2 Linggong Road, Gaoxin District,*

11 *Dalian, Liaoning, China. E-mail: hufangyuan@dlut.edu.cn*

12 <sup>c</sup> *State Key Laboratory of Fine Chemicals, Liaoning Province Engineering Research*

13 *Centre of High Performance Resins, Dalian University of Technology, No.2 Linggong*

14 *Road, Gaoxin District, Dalian, Liaoning, China.*

15 <sup>b</sup> *School of Innovation and Entrepreneurship, Dalian University of Technology, No.2*

16 *Linggong Road, Gaoxin District, Dalian, Liaoning, China*

17

### 18 **Table of content**

19 1. Final modification process for the simulated network.

20 2. Details of the modeling algorithm and the simulation method.

21 3. Simulated models with accessible surface area.

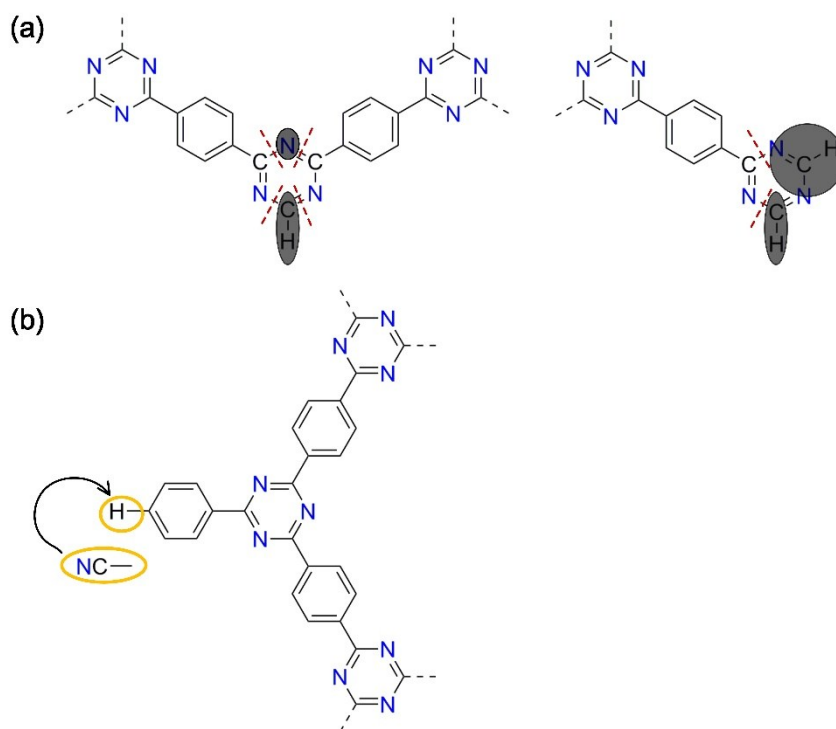
22 4. Simulation details for the structure factors.

23 References

## 1. Final modification process for the simulated network.

2

3 The unlinked building units are removed from the system at first.  
4 Consequently, there remains two kinds of unlinked L2 atoms (displayed in Fig.  
5 S1 (a)) in the system, which will be treated separately. Fig. S1 demonstrates  
6 the modification process diagrammatically. Specifically, when these two kinds  
7 of unlinked L2 atoms are detected in the present system, the atoms in the grey  
8 regions displayed in Fig. S1 will be removed from the system, and then the  
9 remained -CN units are deemed as the unreacted cyano groups. Additionally,  
10 H atoms bonded to the unlinked L1 atoms will be replaced by the cyano groups.  
11 Moreover, the corresponding force field type needs further adjustment  
12 according to the chemical structures and the applied force field. Finally, the  
13 monomers separated from the network would be removed. The whole  
14 modification process is automatically conducted by an in-house Perl script.  
15



16

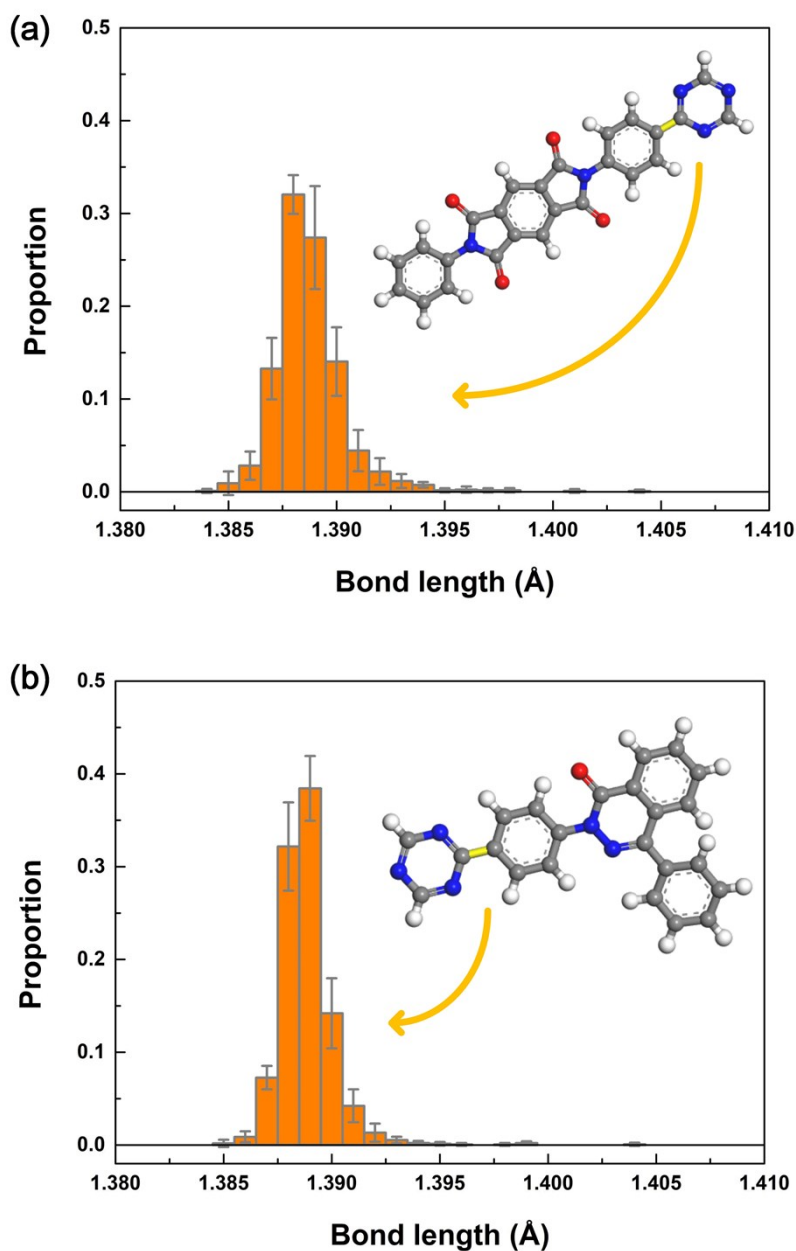
17 Fig. S1 Diagram of the final modification process for the simulated network.

## 1 **2. Details of the modeling algorithm and the simulation** 2 **method.**

3  
4 The initial simulation boxes were generated by the Amorphous Cell module  
5 embedded in BIOVIA Materials Studio 2017R2. 300 monomer building units  
6 and 200 triazine rings (displayed in Fig. 1) are randomly packed in the  
7 simulation cell at a density of 0.4 g/cm<sup>3</sup> for the starting configuration. Therefore,  
8 the desired number of bond formations for the linking cycles is set as 600  
9 herein.

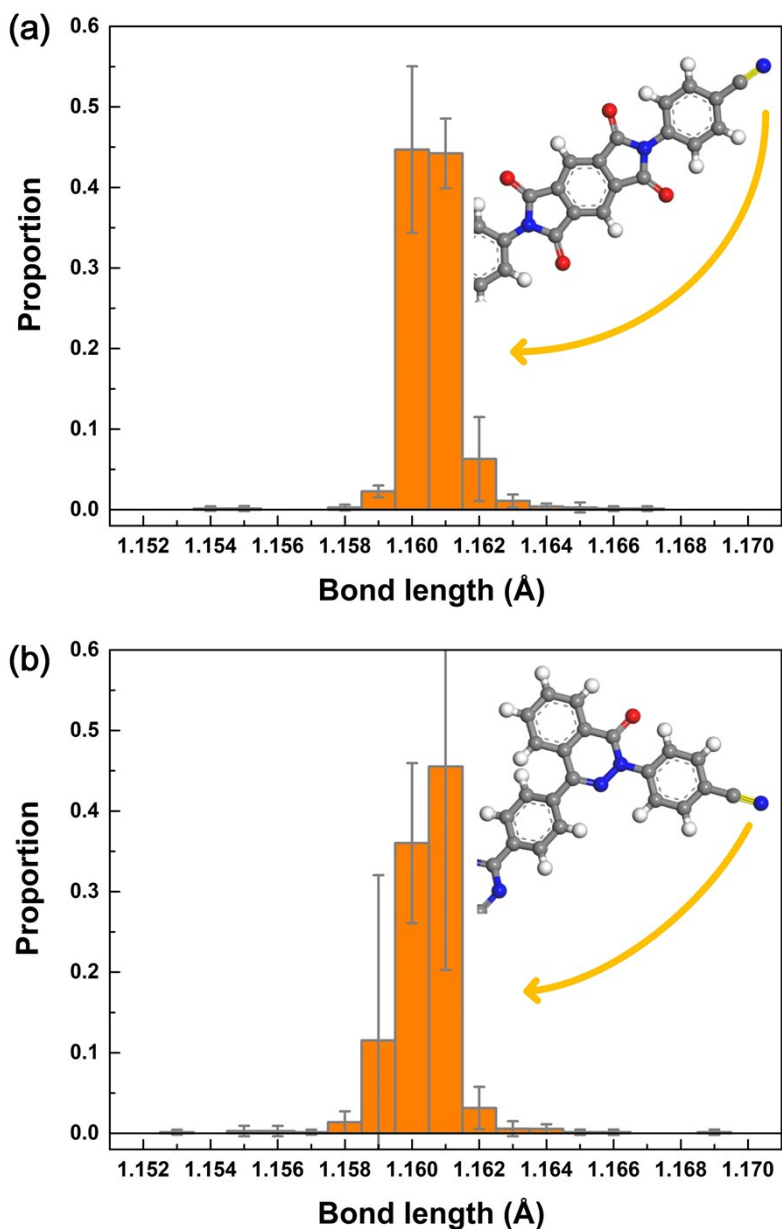
10 Both the geometry optimizations and MD simulations involved in this study  
11 are performed using the Forcite module with COMPASS II force field.<sup>1</sup> The  
12 geometry optimizations during the linking cycles and after the final modification  
13 process consist of 1000 and 2000 steps, respectively, with fine quality settings  
14 and the smart algorithm applied for energy minimization calculations. The  
15 designed geometry optimization steps have been proved to be capable of  
16 optimizing the formed bonds during the linking cycles and the local structures  
17 altered by the final modification process to the realistic structures. Specifically,  
18 the capability of the geometry optimization steps on optimizing and relaxing the  
19 networks is assessed by the length distributions of specific bonds. Fig. S2 and  
20 Fig. S3 show the length distributions of the C-C bonds formed during the linking  
21 cycles and the C-N bonds in the cyano groups generated during the final  
22 modification process (both displayed in the subplots and highlighted in yellow)  
23 after the geometry optimization steps, respectively. The narrow distributions  
24 around the equilibrium bond lengths manifest the efficiency of the designed  
25 geometry optimization steps. The NVT MD simulations during the linking cycles  
26 use the Nosé-Hoover thermostat with a time step of 1 fs at 900 K, which is close  
27 to the temperature of the actual reactions. Specifically, the NVT MD simulations  
28 employed for the searching approaches (i.e., md1 type in Fig. 3) comprise 5000  
29 steps, and the md2 type MD simulations (in Fig. 3) are composed of 10000  
30 steps. The md1 type MD simulation is used to refresh the system for searching  
31 for the potential pair satisfying the bonding criteria during the linking cycles.  
32 Considering the efficiency of the modelling approach and the computational  
33 costs, we set the length of md1 type MD simulation as 5000 steps. Previous  
34 work by Colina *et al* has manifested that the NVT MD steps, although short,  
35 offer adequate time for a slight relaxation of the network during the linking  
36 cycles, which is beneficial to the formation of the realistic lengths of bonds.<sup>2</sup>  
37 Thus, the md2 type MD simulation is inserted into the proposed modelling  
38 approach. Note that the same lengths of the md1 and md2 type NVT MD  
39 simulations have also been employed in the Polymatic algorithm, which has  
40 been successfully implemented for a broad class of polymer networks with  
41 similar size of the simulated systems as ours in this work.<sup>3-5</sup> The MD simulations  
42 during the gradual compression and relaxation process (depicted in Table 1)

1 utilize the Nosé-Hoover thermostat and Berendsen barostat with a time step of  
2 1 fs. Additionally, atom-based summation methods with the cutoff distance of 5  
3 Å and 15 Å are used for the van der Waals interactions for the geometry  
4 optimizations and MD simulations during and at the end of the linking cycles,  
5 respectively. And all electrostatic interactions are calculated by the Particle-  
6 Particle Particle-Mesh (PPPM) method with fine quality settings.  
7 The proposed modeling algorithm is conducted by an in-house Python script,  
8 and the automatic process of searching the systems for the potential linking  
9 pairs and adjustment and modification of the systems is carried out by in-house  
10 Perl scripts, which can be implemented in the Materials Studio package.  
11



12  
13 Fig. S2 Histograms of the length distributions of the C-C bonds formed during the  
14 linking cycles (displayed in the subplot and highlighted in yellow) after the geometry

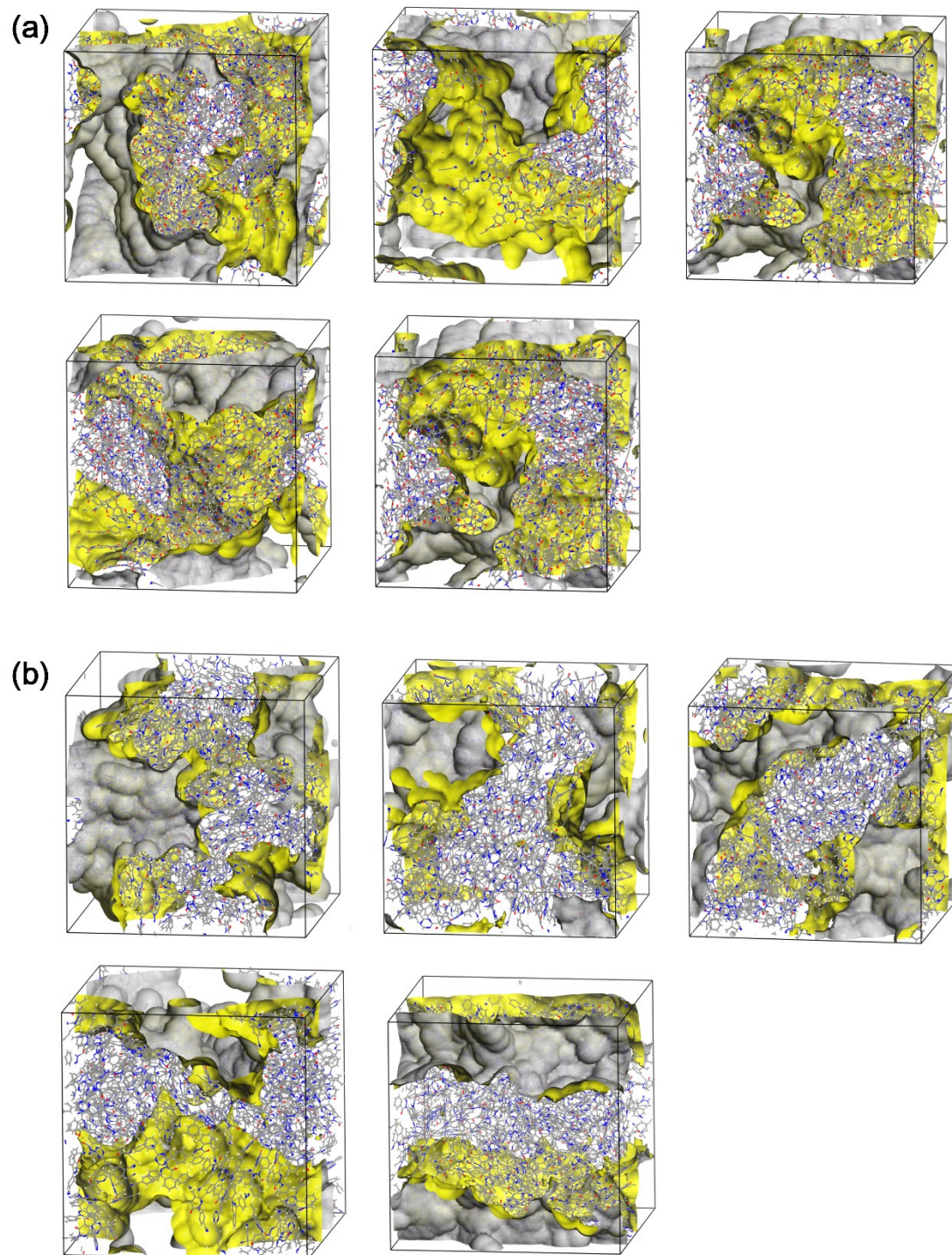
1 optimization steps for (a) MPCF-1 and (b) MPCF-2 simulated models. The results  
2 represent the averages values of the five independent models with error bars  
3 representing the standard deviations.



4  
5 Fig. S3 Histograms of the length distributions of the C-N bonds in cyano groups  
6 generated during the final modification process (displayed in the subplot and  
7 highlighted in yellow) after the geometry optimization steps for (a) MPCF-1 and (b)  
8 MPCF-2 simulated models. The results represent the averages values of the five  
9 independent models with error bars representing the standard deviations.  
10

1 **3. Simulated models with accessible surface area.**

2



3

4 Fig. S4 Simulated accessible surface areas for five independent models of (a) MPCF-1  
5 and (b) MPCF-2.

6

#### 1 **4. Simulation details for the structure factors.**

2 The structure factors for the simulated models were carried out by the ISSAC  
3 software<sup>6</sup> with periodic boundary conditions. The structure factor  $S(q)$  is  
4 provided by the following equation:

$$5 \quad S(q) = 1 + 4\pi\rho \int_0^{\infty} r^2 \frac{\sin qr}{qr} (g(r) - 1) dr, \quad (1)$$

6 where  $g(r)$  represents the radial distribution function. And  $g(r)$  was calculated  
7 by 1000 steps with a smoothing factor of 0.1.



## 1 References

- 2 1. H. Sun, Z. Jin, C. Yang, R. L. Akkermans, S. H. Robertson, N. A. Spenley, S. Miller and S. M.  
3 Todd, *Journal of molecular modeling*, 2016, **22**, 47.
- 4 2. L. J. Abbott and C. M. Colina, *Macromolecules*, 2011, **44**, 4511-4519.
- 5 3. L. J. Abbott, K. E. Hart and C. M. Colina, *Theoretical Chemistry Accounts*, 2013, **132**.
- 6 4. M. E. Fortunato and C. M. Colina, *SoftwareX*, 2017, **6**, 7-12.
- 7 5. G. Kupgan, T. P. Liyana-Arachchi and C. M. Colina, *Polymer*, 2016, **99**, 173-184.
- 8 6. S. Le Roux and V. Petkov, *Journal of Applied Crystallography*, 2010, **43**, 181-185.
- 9